RECENT X-RAY MEASUREMENTS OF THE ACCRETION-POWERED PULSAR 4U 1907+09

J.J.M. in 't Zand

Space Research Organization Netherlands, Sorbonnelaan 2, 3584 CA Utrecht, the
Netherlands; jeanz@sron.ruu.nl

A. Baykal

Physics Department, Middle East Technical University, Ankara 06531, Turkey;
altan@astroa.physics.metu.edu.tr

T.E. Strohmayer[1]

Laboratory for High-Energy Astronomy, NASA - Goddard Space Flight Center, Greenbelt,
MD 20771, U.S.A.; stroh@lheamail.gsfc.nasa.gov

[1]USRA research scientist

ABSTRACT

X-ray observations of the accreting X-ray pulsar 4U 1907+09, obtained
during February 1996 with the *Proportional Counter Array* on the *Rossi X-ray
Timing Experiment* (RXTE), have enabled the first measurement of the intrinsic
pulse period P_{pulse} since 1984: $P_{\text{pulse}} = 440.341^{+0.012}_{-0.017}$ s. 4U 1907+09 is in a
binary system with a blue supergiant. The orbital parameters were solved and
this enabled the correction for orbital delay effects of a measurement of P_{pulse}
obtained in 1990 with Ginga. Thus, three spin down rates could be extracted
from four pulse periods obtained in 1983, 1984, 1990, and 1996. These are
within 8% equal to a value of $\dot{P}_{\text{pulse}} = +0.225$ s yr^{-1}. This suggest that the
pulsar is perhaps in a monotonous spin down mode since its discovery in 1983.
Furthermore, the RXTE observations show transient $\sim$18 s oscillations during a
flare that lasted about 1 hour. The oscillations may be interpreted as Keplerian
motion of an accretion disk near the magnetospheric radius. This, and the
notion that the co-rotation radius is much larger than any conceivable value for
the magnetospheric radius (because of the long spin period), renders it unlikely
that this pulsar spins near equilibrium like is suspected for other slowing
accreting X-ray pulsars. We suggest as an alternative that perhaps the frequent

occurrence of a retrograde transient accretion disk may be consistently slowing the pulsar down. Further observations of flares can provide more evidence of this.

Subject headings: pulsars: individual (4U 1907+09) — stars: neutron — X-rays: stars — binaries

1. Introduction

4U 1907+09 is an X-ray pulsar powered by accretion of wind material from a blue supergiant companion star. It was discovered as an X-ray source by Giacconi et al. (1971) and has been studied using instruments onboard Ariel V (Marshall & Ricketts 1980, MR80), Tenma (Makishima et al. 1984, M84), EXOSAT (Cook & Page 1987, CP87), and Ginga (Makishima & Mihara 1992, Mihara 1995). MR80 first determined the orbital period of the binary at 8.38 days through an analysis of data taken over the course of 5 years (between 1974 and 1980) from a survey instrument on Ariel V with a net exposure time of about $\frac{1}{2}$ year. A folded lightcurve of these data shows a pronounced primary flare and a dimmer and irregular secondary flare. M84 observed 4U 1907+09 with Tenma in 1983 and discovered the pulsar with a pulse period of 437.5 s. Also, through a good time coverage of the binary orbit, they were able to confirm the occurrence of two phase-locked flares. The secondary flare in the Tenma data appears as bright as the primary flare. CP87 discuss EXOSAT data with a small though reasonably uniform coverage of the orbit. They also find evidence for a phase-locked primary and secondary flare. Through combining Tenma and EXOSAT data, they were able to determine the binary orbit most accurately and found an eccentricity of $0.16^{+0.14}_{-0.11}$. A measurement of the pulse period revealed an average spin down rate of $+0.23$ s yr^{-1} since the Tenma measurement 270 d earlier. 4U 1907+09 was observed with Ginga in 1990. Makishima & Mihara (1992) report a cyclotron feature at 21 keV found during these observations. Mihara (1995) measured the pulse period using the Ginga data, without correcting for the binary orbit its value was determined to be 439.47 s. Sadeh & Livio (1982), using data from the HEAO A-1 instrument, report the occurrence of 15 ms oscillations during 4 out of 20 scans of the source each lasting about 10 s. The oscillation period was seen to change during each scan.

In February 1996, 4U 1907+09 was observed with the narrow-field instruments on the *Rossi X-ray Timing Explorer* (RXTE). A previous paper (In 't Zand, Strohmayer & Baykal, 1997, ISB97) reported a frequent occurrence of complete dips in the pulsar signal with durations between a few minutes and $1\frac{1}{2}$ hrs as found in these data. In the current

paper we report about the same data but concentrate on variability on time scales shorter than or equal to the pulse period. We discuss the pulse period and its history since 1983 and present evidence for the occurrence of transient oscillations. These timing diagnostics enable one to address interesting questions about the presence of an accretion disk and the angular momentum transfer in the binary. Furthermore, we briefly discuss the general spectral trend as a function of pulse phase.

2. Observations

RXTE-PCA (Zhang et al. 1993) consists of five identical proportional counters that are co-aligned to the same point in the sky. Collimators limit the field of view (FOV) to 1 square degree. The total geometric collecting area is approximately 6250 cm^2, the effective sensitive photon energy range is from 2 to 60 keV. The satellite is in a low-earth orbit so that long observations may be broken up by earth occultations and passes through the South Atlantic Anomaly.

RXTE-PCA observed 4U 1907+09 during 4 observation runs which are detailed in Table 1 and total 79.4 ks. The mode of data collection for the four observation runs was event data with 64 energy channels resolution over the full bandpass and a time resolution of 16 μs. No detector identification bits were telemetred. At the time of the observations, the on-board gain correction algorithm was temporarily turned off (Jahoda et al. 1996). The gains of the 5 PCA detectors are slightly different. Whenever we quote intensities in a certain energy range, we refer to the energy range consistent with the channel setting of detector "PCU0". We note that the gains of the other detectors are deviating by less than 0.1 keV at the low end to at most 2 keV at the high end of the range.

There are a number of known contributors to the X-ray background in our measurements: the cosmic diffuse background, the diffuse galactic ridge emission and the supernova remnant W49B. The latter two have not been accurately imaged yet in our bandpass. This forces us to employ a simplified background subtraction procedure which has been detailed in ISB97: the X-ray background is defined as the residual emission found during dip times when there is no apparent pulsed emission. Using this background implies two assumptions: if there is residual emission from 4U 1907+09 we disregard that and assume it is constant, and there is no other variable source in the background. The last assumption seems reasonable given the mentioned contributors, certainly on the time scale of the observations. With regards to residual emission from 4U 1907+09, we can only note that estimates of the different contributions are prone to systematic errors but suggest that residual emission is at a level less than 2% of the average 4U 1907+09 intensity in the 2 to

15 keV band (ISB97).

3. The X-ray light curve

Figure 1 shows the time history of the raw countrate of the RXTE-PCA observations on 4U 1907+09. Apart from the dips, the pulsar signal with a period of about 440 s is obvious. The pulse profile is very variable. It can change from pulse to pulse or even within one pulse. The time history shows a flare at Feb. 23.07 when the net 2 to 15 keV intensity rises up by an order of magnitude to about 0.1 Crab units. Given the newly determined orbital period (§ 4) this flare occurs 543.99±0.04 orbital periods after the secondary and 544.44±0.04 orbital periods after the primary flare as observed with Tenma in August and September of 1983 (M84) which are the most recent timing reports of flares. The identification of the flare on Feb. 23.07 with the secondary flare seems unambiguous and, therefore, we confirm the recurrence of a phase-locked secondary flare. It is interesting to note that the orbital phase of the flare (see Table 1) places it near to the time of apastron of the binary. The intensity of the flare is, in 2 to 30 keV, about twice as high as the one measured with Tenma (M84). This is not unexpected. The secondary flare has been seen to vary from insignificant to as bright as the primary flare (MR80). We note that the observed flare may actually be only part of a more extended secondary flare which could have been missed because of the sparsity of the RXTE coverage. The Tenma observation of the secondary flare suggests the flare may last 0.3 days, the associated uncertainty in the epoch has been included in the above-mentioned uncertainty of the number of orbital periods since the Tenma-observed flares.

4. Timing analysis of the pulse signal

An initial estimate of the pulse period was obtained by folding the 2 to 15 keV time history on a number of statistically independent trial periods (Leahy et al. 1983) in the range 430 to 450 s. Only data outside the intensity dips were used and photon arrival times were corrected into those for the solar system barycenter. The highest χ^2 value was found for a period of 440.4 s (figure 2).

In order to accurately determine the pulse period as well as the binary orbit a set of 19 pulse arrival times was generated, one pulse arrival time for each XTE orbit when 4U 1907+09 is not in a dip. This was done by folding the time history data into one average pulse for each RXTE orbit, folding *all* time history data into one master pulse, and

cross correlating the master pulse with each average pulse to find the pulse arrival time for each average pulse. Average profiles rather than individual pulses were used to minimize systematic effects due to the sometimes strong changes in the profile from pulse to pulse which are supposedly due to variability in the accretion rate (ISB97).

As an alternative to control the pulse profile variability we have used the method of pulse wave filtering as proposed by Deeter & Boynton (1985, see also Boynton et al. 1986). In this method pulse profiles are expressed in terms of harmonic series and cross correlated with the average pulse profile ('master pulse'). The maximum value of the cross correlation is analytically well-defined and does not depend on the phase binning of the pulses. The short term sharp fluctuations of pulses are naturally filtered by a cut off of higher harmonics. The pulse arrival times obtained through this method gave statistically the same results as those obtained through the above-mentioned method.

In order to increase the accuracy of the orbital solution (in particular the orbital period), the pulse arrival times were combined with the pulse delay-time data from Tenma observations as published graphically by M84.

We modeled the data with an eccentric orbit with parameters that have not changed since the Tenma observations in September 1983 and with a pulse period which is constant throughout our RXTE observations. We determined the parameters by testing the model against the data using Pearson's χ^2 test on a grid of parameter values sufficiently sampled to detect significant changes in χ^2 and with a range to sufficiently enclose the allowed parameter values. The parameters are the pulse period P_{pulse} at the time of the RXTE observations, the orbital period P_{orb}, the epoch of mean longitude 90 degrees $T_{\pi/2}$ (i.e., one quarter of the orbital period after the time of ascending node when the neutron star crosses the sky tangent plane through the barycenter moving away from the observer), the longitude of periastron ω (i.e., with respect to the ascending node), the eccentricity e, and the length of the projected semi-major axis $a_{\mathrm{x}} \sin i/c$. The grid ranges and sample frequencies were found iteratively, going from a rough to a sufficiently fine grid. We choose this grid-search method to be able to determine the uncertainty of the solution with any arbitrary confidence level. The χ^2 values were calculated in the pulse delay-time domain. On the one hand this enables the inclusion of the Tenma data that have not been published in the pulse arrival-time domain, on the other hand this precludes the determination of P_{pulse} during the Tenma observations. We fixed the error in the pulse delay times at 8 s. This value was suggested by the uncertainty of the harmonics in the pulse wave filtering analysis of the RXTE data and was the value M84 applied for the Tenma data.

The results of modeling the timing data are presented in Table 2. The quoted error intervals are the projections of the 68% confidence level region onto each of the 6 parameter

axes. Since some parameters are very dependent, the actual solution is confined within a much smaller space than that of the 6-dimensional cube dictated by the quoted errors. The errors are, therefore, conservative. For the purpose of easy comparison with orbital solution by others, we have also included the single-parameter 1σ errors in Table 2. Figure 3 presents a plot of the orbital model versus the data in terms of delay times with respect to the binary barycenter.

The orbital solution provides a means to correct the pulse period as determined with Ginga in 1990 (Mihara 1995) for the orbital motion of the neutron star in the binary system. The Ginga observations were performed for a duration of 14 hours (this is 0.07 in phase) at a mean time of MJD 48156.60. This is 0.10 orbital periods after the epoch of ascending node where the orbital Doppler shift is +0.28 s per pulse period with an uncertainty of about 0.01 s per pulse period. Therefore, the corrected pulse period is 439.19 s.

We find a pulse period at the time of the RXTE observations of $440.341^{+0.012}_{-0.017}$ s. This completes a total of four measurements of the pulse period and 3 measurements of the pulse period derivative since 1983. These values, tabulated in Table 3, imply an interesting finding: the pulsar appears to be spinning down with a close to constant derivative. The three values are within 8% of a mean value of $\dot{P}_{\mathrm{pulse}} = +0.225$ s yr^{-1}.

As mentioned, we assumed that over the course of 12 years there is no noticeable change in P_{orb}, ω and the orbit inclination angle i. For P_{orb}, we can confirm this with reasonable accuracy because the value we find is, within error margins, equal to what was found by CP87 between the Tenma and EXOSAT measurements (8.3745 ± 0.0042 days). For ω, the uncertainty, typically 20 degrees, is simply too large to be at all able to measure likely values for the change (for a detailed analysis of apsidal advance in the similar system Vela X-1, see Deeter et al. 1987). The same argument holds for the sensitivity towards measuring changes in i.

The photon arrival times were folded with the pulse period after correction for the earth's motion around the sun, RXTE's motion around the earth and the binary motion of the pulsar. The resultant pulse profile is presented in figure 4 for 6 photon energy bands up to 38 keV. Above this energy no pulsed emission was detected, as revealed by a Fourier analysis (figure 5). The pulse profiles are expressed in units of average 4U 1907+09 intensity per band. The background in each band was determined as discussed in ISB97 (see §2). The pulse profile consists of two peaks with a deep and a shallow minimum in between that are close to 0.5 in pulse phase apart. The pulse profile looks similar to that observed more than a decade before with Tenma and EXOSAT in similar energy bands (M84 and CP87). It is rather insensitive to energy between 2 and 20 keV although subtle dependencies are noticeable, particularly in the second peak. There is a dramatic change of the pulse profile

at around 20 keV. Basically, the first pulse disappears above that energy and the shape of the other one changes. The modulation depth is roughly the same in all bands. The energy dependency of the pulse profile appears similar to that observed from Cen X-3 with Ginga (Nagase et al. 1992).

5. Transient 18 s oscillations

Visual inspection of the X-ray lightcurve on second timescales during the flare at Feb. 23.07 suggests that there is a variety of non-Poissonian variability present during the flare. For example, figure 6 shows the lightcurve of a 500 second interval near the peak of the flare. Fluctuations in the countrate as large as several hundred counts s^{-1} are obvious in this lightcurve. To further quantify this short timescale variability (i.e., shorter than a pulse period) we computed Fourier power spectra for the time intervals encompassing the flare. The power spectrum of a 1024 second interval beginning 300 seconds prior to that shown in figure 6 is displayed in figure 7. There are a number of conspicuous peaks in this power spectrum in the range from 0.02 to 0.06 Hz. There is also clearly a broadband noise component increasing toward lower frequencies, as the mean power is significantly above 2 (the mean expected for purely poisson fluctuations) extending above 0.2 Hz. One of the most prominent peaks is at 0.055 Hz, or a period of 18.2 s. These 18 s oscillations can actually be seen with the eye in figure 6. To investigate further we performed an epoch folding period search in the vicinity of 18 s. The results are shown in figure 8, and there is an obvious peak centered at 18.2 s. To determine the average amplitude of the oscillations, we folded the 1024 s of data on the best-fit period of 18.2 seconds . We then fit a model including a constant countrate plus a sinusoid to the folded data. Figure 9 shows the resulting background subtracted lightcurve and the best-fit sinusoidal model. The χ^2 per degree of freedom is formally a bit high, 1.8, but for estimating the amplitude of the oscillation the sinusoidal fit is sufficient. From this analysis we obtain an average oscillation amplitude of $4.4 \pm 0.3\%$, where the amplitude is defined as the ratio of the sinusoidal to constant countrate components. We also investigated the dependence on photon energy of both the pulsation amplitude and pulse profile, but found no significant energy dependence.

The 18 s oscillations are not persistent, rather, they are confined to an approximately 1000 s interval centered near the peak of the flare. To investigate the transient nature of the 18 s oscillation we computed a dynamic power spectrum by calculating power spectra from 500 second intervals with a new interval beginning every 50 seconds. The resulting power spectra are not independent, since the data segments overlap, however, this method identifies the range of times for which the 18 s oscillations are present. The resulting

dynamic spectrum is shown in the top panel of figure 10. The 0.055 Hz oscillations are clearly present from about 200-1200 seconds, and this is the only epoch in which we detected such oscillations. During the time that the oscillations are present there is no strong evidence for significant frequency drift, this gives a lower limit to the Q-value for the oscillation of $Q = (1000\text{s}/18.2\text{s}) = 55.6$ (Q is the so-called quality factor which measures the number of oscillations that will pass before a substantial fraction of the energy of the oscillator is dissipated, Q is inversely proportional to the bandwidth or spectral purity of the oscillation).

To investigate the nature of the broadband noise we computed an average FFT power spectrum from two successive orbits during the flare, for a total of 6250 seconds of data. The resulting average power spectrum is shown in figure 11. We fit a power law model $P = K\nu^{-\alpha}$ to 51 frequency bins in the 0.02 to 4 Hz frequency range. We did not fit below 0.02 Hz because there the power spectrum is dominated by the pulsed signal and its harmonics. The power law model with $K = 0.41 \pm 0.07$ and $\alpha = 1.36 \pm 0.06$ provides an acceptable fit, with a $\chi^2/\text{d.o.f.} = 39/49 \approx 0.8$. The integrated power from 0.02 to 4 Hz corresponds to an amplitude (rms) of about 8.2%.

We note that we have searched for pulsations at higher frequencies and failed to find any. No pulsations are present like were reported by Sadeh & Livio (1982) at a period of around 15.3 ms. During the flare we find an upper limit for the amplitude of 0.5% as compared to the amplitude of 12% at which pulsations were seen by Sadeh & Livio.

6.   Discussion

Quasiperiodic oscillations (QPO) with frequencies in the 10 - 200 mHz range have been observed from 7 other X-ray pulsars. Among these, A0535+26 (Finger, Wilson, & Harmon 1996), X1626-67 (Shinoda et al. 1990), Cen X-3 (Takeshima et al. 1991), V0332+53 (Takeshima et al. 1994), X0115+63 (Soong & Swank 1989), and SMC X-1 (Angelini 1989) all have QPO frequencies in the 0.062 to 0.1 Hz regime, similar to the 0.055 Hz transient oscillation from 4U 1907+09 described above. The $\approx 4\%$ amplitude (rms) of the 18 s oscillation is also similar to the amplitudes of QPO from other X-ray pulsars (see Takeshima et al. 1994; and Angelini, Stella & Parmar 1989), however, QPO detected in these sources typically are broader, with Q-values of order a few compared to about 50 for the 18 s oscillation in 4U 1907+09.

To date, almost all models for QPO in X-ray pulsars postulate the existence of an accretion disk as the site of QPO production. In the case of QPO from A0535+26 this

is supported by the observed correlation of the QPO frequency and spin-up rate (Finger, Wilson, & Harmon 1996), strongly suggesting the transfer of angular momentum from accretion disk to neutron star. Thus, one possibility is that the 18 s oscillations reveal the presence of a transient accretion disk during the flare.

Assuming that the 18 s oscillation in 4U 1907+09 is related to orbital motion, either via a beat frequency model (BFM, Lamb et al. 1985; Alpar & Shaham 1985), or a Kepler frequency model (KFM, van der Klis et al. 1987), then the inferred radius of material in a putative disk is $R_{\rm d} = (GM/4\pi^2\nu_{QPO}^2)^{1/3} \approx 1.2 \times 10^4$ km, for a 1.4 $M_\odot$ neutron star. This is nearly an order of magnitude smaller than the co-rotation radius $R_{\rm c} = 9.6 \times 10^4$ km for this object. We can rougly estimate the size of the neutron star magnetosphere from the expression for the Alfvén radius assuming spherical accretion (e.g., Ghosh & Lamb 1991),

$$
\begin{aligned}
R_{\rm m} \;=\; & 2.4 \times 10^3 (M/1.4\ M_\odot)^{1/7} \times \\
& (B/2.5 \times 10^{12} G)^{4/7} \times \\
& (R/10^6\ {\rm cm})^{10/7} \times \\
& (L_{\rm x}/3.1 \times 10^{37} {\rm ergs\ s}^{-1})^{-2/7} \quad {\rm km.}
\end{aligned}
\tag{1}
$$

Studies of the optical counterpart, discovered by Schwartz et al. (1972), reveal that the distance to 4U 1907+09 is between 2.4 and 5.9 kpc (Van Kerkwijk et al. 1989). Assuming the distance is 4 kpc, the average non-absorbed luminosity of 4U 1907+09 during non-dip and non-flare periods and within the studied energy range is 1×10^{36} erg s^{-1} (ISB97). During the flare the luminosity increases up to 4×10^{36} erg s^{-1}. For a flare X-ray luminosity of 4×10^{36} ergs/s, a magnetic field $B = 2.5 \times 10^{12}$ G and a stellar mass and radius of 1.4 $M_\odot$ and 10 km respectively, $R_{\rm m} \approx 4300$ km. Although this number is rather uncertain it suggests that the disk can certainly penetrate close enough to the star to account for the 18 s oscillations as an orbital phenomenon associated with an accretion disk. Although the accretion disk interpretation seems plausible, further observations, particularly in the vicinity of the flare will be required to confirm this interpretation.

Long-term measurements of the behavior of the spin period for a selection of 15 accreting X-ray pulsars (Bildsten et al., 1997) show that three known pulsars appear to exhibit systematic spin-down evolution for at least 5 years: GX1+4 ($P/\dot{P} \approx$90 yrs), 4U 1626-67 ($P/\dot{P} \approx 5 \times 10^3$ yrs) and Vela X-1 ($P/\dot{P} \approx 6 \times 10^3$ yrs). Generally, this behavior is attributed to low accretion rates that bring the magnetospheric radius $R_{\rm m}$ close to the co-rotation radius $R_{\rm c}$ (Ghosh & Lamb 1979a, 1979b; Wang 1987, 1995; Anzer & Börner 1980; Lovelace, Romanova & Bisnovatyi-Kogan 1995). However, for 4U 1907+09 this is an unlikely scenario because the magnetospheric radius is hard to bring out to such a large co-rotation radius unless either the magnetic field is of unlikely order 10^{14} G or the distance

is of order 0.5 kpc which is at least 5 times lower than studies of the optical counterpart suggest.

The putative disk supports the notion that the magnetospheric radius is substantially smaller than the co-rotation radius. Moreover, a disk can provide an alternative explanation to the observed spin down if this transient disk is rotating in an opposite sense to the pulsar spin. Such a disk can provide the necessary torque to explain the spin down rate. If all accreted mass supplies its angular momentum at a radius R_d the expected torque on the neutron star is $N_{\mathrm{char}} = \eta \dot{M}(GMR_d)^{1/2}$ where $\eta < 1$ is the duty cycle of the transient disk. If we assume that all the liberated potential energy of the accreted mass during the flare is transformed into radiation and the flare luminosity is $3.2 \times 10^{35} D_{\mathrm{kpc}}^2$ erg s^{-1}, then $N_{\mathrm{char}} = 2.5 \times 10^{22} \eta D_{\mathrm{kpc}}^2 R_d^{1/2}$. For $R_d = 1.2 \times 10^4$ km this becomes $N_{\mathrm{char}} = 8.6 \times 10^{32} \eta D_{\mathrm{kpc}}^2$ g cm^2. The observed absolute value of the torque is $N_{\mathrm{obs}} = 2\pi I |\dot{\nu}|$ where I is the moment of inertia and $\dot{\nu} = -3.7 \times 10^{-14}$ Hz s^{-1} (equivalent to $\dot{P} = +0.225$ s yr^{-1}). If $I = 10^{45}$ g cm^2 (generic value for a neutron star of radius 10 km and mass 1.4 M$_\odot$), $N_{\mathrm{obs}} = 2.3 \times 10^{32}$ g cm^2. If $N_{\mathrm{obs}} = N_{\mathrm{char}}$ and $2.4 < D_{\mathrm{kpc}} < 5.9$, then $0.008 < \eta < 0.05$. Therefore, the putative retrograde transient accretion disk can provide the torque to spin down the pulsar if it lasts on average on the order of a few percent of the time. We observed a duty cycle of about 1000 s out of an orbital period of 8.4 d which is an order of magnitude too small. However, the coverage of our observations is limited and also the flare might, averaged over many orbits, have a larger duty cycle. This is confirmed by Tenma observations which suggest a duration of 0.3 d for one flare (M84). We conclude that the putative retrograde accretion disk could possibly supply enough negative torque to spin down the pulsar.

The suggestion of a retrograde accretion disk being responsible for an extensive spin down period has recently been revisited in the case of the disk-fed AXP GX1+4 by Chakrabarti et al. (1997) in order to have an elegant explanation for a positive correlation between luminosity and negative torque. Our need for a retrograde accretion disk in the wind-fed 4U 1907+09 is motivated by a co-rotation radius which is clearly much larger than the magnetospheric radius.

4U 1907+09 is in several ways similar to Vela X-1: the spin periods are both of order several hundred seconds (440 s for 4U 1907+09 and 283 s for Vela X-1), the orbital periods are of order 8 days (8.38 d for 4U 1907+09 and 8.96 d for Vela X-1), and both have recently been found to show long periods of systematic spin down (e.g., Bildsten et al. 1997 for Vela X-1). Previously, the occasional spin-down periods in Vela X-1 have been attributed to the presence of a disk with an inner edge close to the co-rotation radius (Nagase 1989), with the note that this implies relatively large magnetic fields (surface fields of order 10^{13} G).

We suggest that, since this reasoning goes awry in the case of 4U 1907+09, this conclusion may be invalid for Vela X-1 as well. An important difference between both systems is that Vela X-1 shows much more spectral variability and pronounced iron lines. This may be due to a difference in angle of sight of the binary orbit, a difference in the spatial distribution of the wind from the companion star, and/or a somewhat different eccentricity.

There is, as compared with some other AXPs, moderate spectral variability within the pulse profile. Basically the pulse profile shows two peaks below and one peak above $\sim$20 keV. This is somewhat similar to what has been observed from the much more luminous disk-fed AXP Cen X-3 and may be associated with two magnetic poles which have either different physical circumstances or are viewed on at different angles by the observer. A modeling of the pulse profile, similar to studies performed by Bulik et al. (1995) and beyond the scope of this paper, may provide more definite conclusions about this.

Since its discovery by MR80, the occurrence of two flares per orbit has been difficult to reconcile with the identification of the companion as a supergiant high-mass star (e.g., Van Kerkwijk et al. 1989, ISB97). It has always been thought that these stars do not have a circumstellar disk like is presumed for Be stars. However, recently evidence is mounting that in hot supergiants in the upper part of the H-R diagram axial symmetry may play an important role (e.g., Zickgraf et al. 1996 and references therein). Also, recently another wind-fed AXP with a supergiant companion has been shown to consistently display two flares per orbit: GX 301-2 (Pravdo et al. 1995; Chichkov et al. 1995; Koh et al. 1997). This again supports the notion that the wind from the companion is not isotropic but that the mass flux is enhanced along the equatorial plane. The two flares then may be caused by the neutron star traversing this plane twice per orbit in a sufficiently inclined orbit. It is interesting to note in this context that GX 301-2 (Sato et al. 1986) and 4U 1907+09 have the highest eccentricity of the group of supergiant high-mass XRBs, perhaps these systems are not yet in a tidal equilibrium. Perhaps even the spin orientation of the neutron star differs by more than 90º from the orbital motion orientation. However, at the moment this is mere speculation.

7. Conclusion

We have determined the pulse period of 4U 1907+09 at a recent epoch and find that the pulsar has spun down on average by 0.225 s yr^{-1} since the pulsar's discovery in 1983. Three measurements of the spin down rates during intermediate time interval spanning between 1 year and 6 years are consistent within 8% of this value. This suggests a remarkable monotonous spin down trend during about 12 years. Furthermore, we find the

occurrence of 18 s oscillations for 10^3 s of a flare with a high Q value hinting at an accretion disk. The indication that the magnetospheric radius is much smaller than the co-rotation radius, the observed long and constant spin down trend and the occurrence of transient oscillations suggest that possibly a recurrent transient accretion disk counter rotates the neutron star and, through transfer of angular momentum, slows the pulsar down. This suggestion needs to be confirmed by at least detailed multiple observations of flares which are almost certainly recurring every orbital period.

REFERENCES

Alpar, M. A., & Shaham, J. 1985, Nature, 316, 239

Angelini, L. 1989, in Proc. 23d ESLAB Symp., Two Topics in X-ray Astronomy, Vol. 1, ed. N. White (Garching: ESA), 81

Angelini, L., Stella, L., & Parmar, A. N. 1989, ApJ, 346, 906

Anzer, U., Börner, G. 1980, A&A, 83, 133

Bildsten, L., Chakrabarti, D., Chiu, J., Finger, M.H., Koh, D.T., Nelson, R.W., Prince, T.A., Rubin, B.C., Scott, D.M., Stollberg, M., Vaughan, B.A., Wilson, C.A., Wilson, R.B. 1997, ApJS, 113, 367

Boynton, P.E., Deeter, J.E., Lamb, F.K., Zylstra, G. 1986, ApJ, 307, 545

Bulik, T., Riffert, H., Meszaros, P., Makishima, K., Mihara, T., Thomas, B. 1995, ApJ, 444, 405

Chakrabarty, D., Bildsten, L., Finger, M.H., Grunsveld, J.M., Koh, D.T., Nelson, R.W., Prince, T.A., Vaughan, B.A., Wilson, R.B. 1997, ApJ, 481, L101

Chichkov, M.A., Sunyaev, R.A., Lapshov, I.Y., Lund, N., Brandt, S., Castro-Tirado, A. 1995, PAZh, 21, 491

Cook, M.C., Page, C.G. 1987, MNRAS, 225, 381

Deeter, J.E., Boynton, P.E. 1985, Proc. Inuyama workshop on Timing Analysis of X-ray Sources, eds. S. Hayakawa & F. Nagase

Deeter, J.E., Boynton, P.E., Lamb, F.K., Zylstra, G. 1987, ApJ, 314, 634

Finger, M. H., Wilson, R. B., & Harmon, B. A. 1996, ApJ, 459, 288

Giacconi, R., Kellogg, E., Gorenstein, P., Gursky, H., Tananbaum, H. 1971, ApJ, 165, L27

Ghosh, P., Lamb, F.K. 1979a, ApJ, 232, 259

Ghosh, P., Lamb, F.K. 1979b, ApJ, 234, 296

Ghosh, P., Lamb, F.K. 1991, in "Neutron Stars Theory and Observation", eds. J. Ventura and D. Pines, NATO ASI Series 43, 363

Inoue, H. 1985, Space Sci. Rev., 40, 317

In 't Zand, J.J.M., Strohmayer, T.E., Baykal, A. 1997, ApJ, 479, L47

Jahoda, K., J.J. Swank, Giles, A.B., Stark, M.J., Strohmayer, T., Zhang, W. 1996, Proc. SPIE, 2808, 59

Koh, D.T., Bildsten, L., Chakrabarti, D., Nelson, R.W., Prince, T.A., Vaughan, B.A., Finger, M.H., Wilson, R.B., Rubin, B.A. 1997, ApJ, 479, 933

Lamb, F. K., Shibazaki, N., Alpar, M. A., & Shaham, J. 1985, Nature, 317, 681

Leahy, D.A. Darbro, W., Elsner, R.F., Weisskopf, M.C., Sutherland, P.G., Kahn, S., Grindlay, J.E. 1983, ApJ, 266, 160

Lovelace, R.V.E., Romanova, M.M., Bisnovatyi-Kogan, G.S. 1995, MNRAS, 275, 244

Makishima, K., Kawai, N., Koyama, K., Shibazaki, N., Nagase, F., Nakagawa, M. 1984, PASJ, 36, 679

Makishima, K., Mihara, T. 1992, in "Frontiers of X-ray Astronomy", Proceedings of the Yamada Conference XXVIII, eds. Y. Tanaka & K. Koyama (Universal Academy Press: Tokyo), 23

Marshall, N., Ricketts, M.J. 1980, MNRAS, 193, 7P

Mihara, T. 1995, Ph.D. thesis, University of Tokyo

Nagase, F. 1989, PASJ, 41, 1

Nagase, F., Corbet, R.H.D., Day, C.S.R., Inoue, H., Takeshima, T., Yoshida, K., Mihara, T. 1992, ApJ, 396, 147

Pravdo, S.H., Day, C.S., Angelini, L., Harmon, B.A., Yoshida, A., Saraswat, P. 1995, ApJ, 454, 872

Sadeh, D., Livio, M. 1982, ApJ, 258, 770

Sato, N. Nagase, F., Kawai, N., Kelley, R.L., Rappaport, S., White, N.E. 1986, ApJ, 304, 241

Schwartz, D.A., Bleach, R.D., Boldt, E.A., Holt. S.S. Serlemitsos, P.J. 1972, ApJ, 173, L51

Shinoda, K., *et al.* 1990, PASJ, 42, L43

Soong, Y. & Swank, J. H. 1989, in Proc. 23d ESLAB Symp., Two Topics in X-ray Astronomy, Vol. 1, ed. N. White (Garching: ESA), 617

Takeshima, T., *et al.* 1991, PASJ, 43, L43

Takeshima, T., Dotani, T., Mitsuda, K., & Nagase, F. 1994, ApJ, 436, 871

van der Klis, M., Jansen, F., van Paradijs, J. P., Lewin, W. H. G., Trumper, J., & Sztajno, M. 1987, ApJ, 313, L19

Van Kerkwijk, M.H., Van Oijen, J.G.J., van den Heuvel, E.P.J. 1989, A&A, 209, 173

Wang, Y.M. 1987, A&A, 183, 257

Wang, Y.M. 1995, ApJ, 449, L153

Zhang, W., Giles, A.B., Jahoda, K., Soong, Y. Swank, J.H., Morgan, E.H. 1993, Proc. SPIE, 2006, 324

Zickgraf, F.-J., Humphreys, R.M., Lamers, H.J.G.L.M., Smolinski, J., Wolf, B., Stahl, O. 1996, A&A, 315, 510

Table 1: RXTE observation log of 4U 1907+09

Observation run	1	2	3	4
Dates (Feb. 1996, U.T.)	17.73-18.15	19.67-20.10	21.60-22.08	23.02-23.42
Orbital phases[a]	0.55-0.60	0.78-0.84	0.01-0.07	0.18-0.23
Orbital phases[b]	0.85-0.90	0.08-0.14	0.31-0.37	0.48-0.53
Exposure time (s)	19442	19911	20261	19775
Time span (s)	36093	37601	41658	33457

[a]Based on epoch of maximum distance between neutron star and earth

[b]Based on epoch of periastron

Table 2: The binary orbit and pulse period of 4U1907+09 from 1983 Tenma and 1996 RXTE-PCA measurements

Parameter	Symbol	Value	68% confidence region	Single parameter 1σ error
Orbital period	P_{orb}	8.3753 days	$+0.0003$ -0.0002	0.0001
Eccentricity	e	0.28	$+0.10$ -0.14	0.04
Orbital epoch	$T_{\pi/2}$	MJD 50134.76	$+0.16$ -0.20	0.06
Longitude of periastron	ω	330 degrees	$+20$ -20	7
Projected semi-major axis length	$a_{\mathrm{x}} \sin i/c$	83 lt-s	$+4$ -4	2
Pulse period	P_{pulse}	440.341 s	$+0.012$ -0.017	0.006

Table 3: History of P_{pulse} measurements for 4U 1907+09

Mean time Date	(MJD)	Satellite	Reference	P_{pulse} (s)	Derivative[a] (s yr^{-1})
Aug./Sept. 1983	45576	Tenma	M84	437.483±0.004	—
May/June 1984	45850	EXOSAT	CP87	437.649±0.019	0.22±0.03
Sep. 1990	48156.6	Ginga	Mihara 1995	439.19±0.02[b]	0.244±0.005
Feb. 1996	50134	RXTE	this paper	440.341±0.014	0.212±0.004

[a]The pulse period derivative is calculated from the difference in P_{pulse} with respect to the previous observation in this table.

[b]This value was corrected for delays from binary motion in the present work. The uncertainty is an estimate.
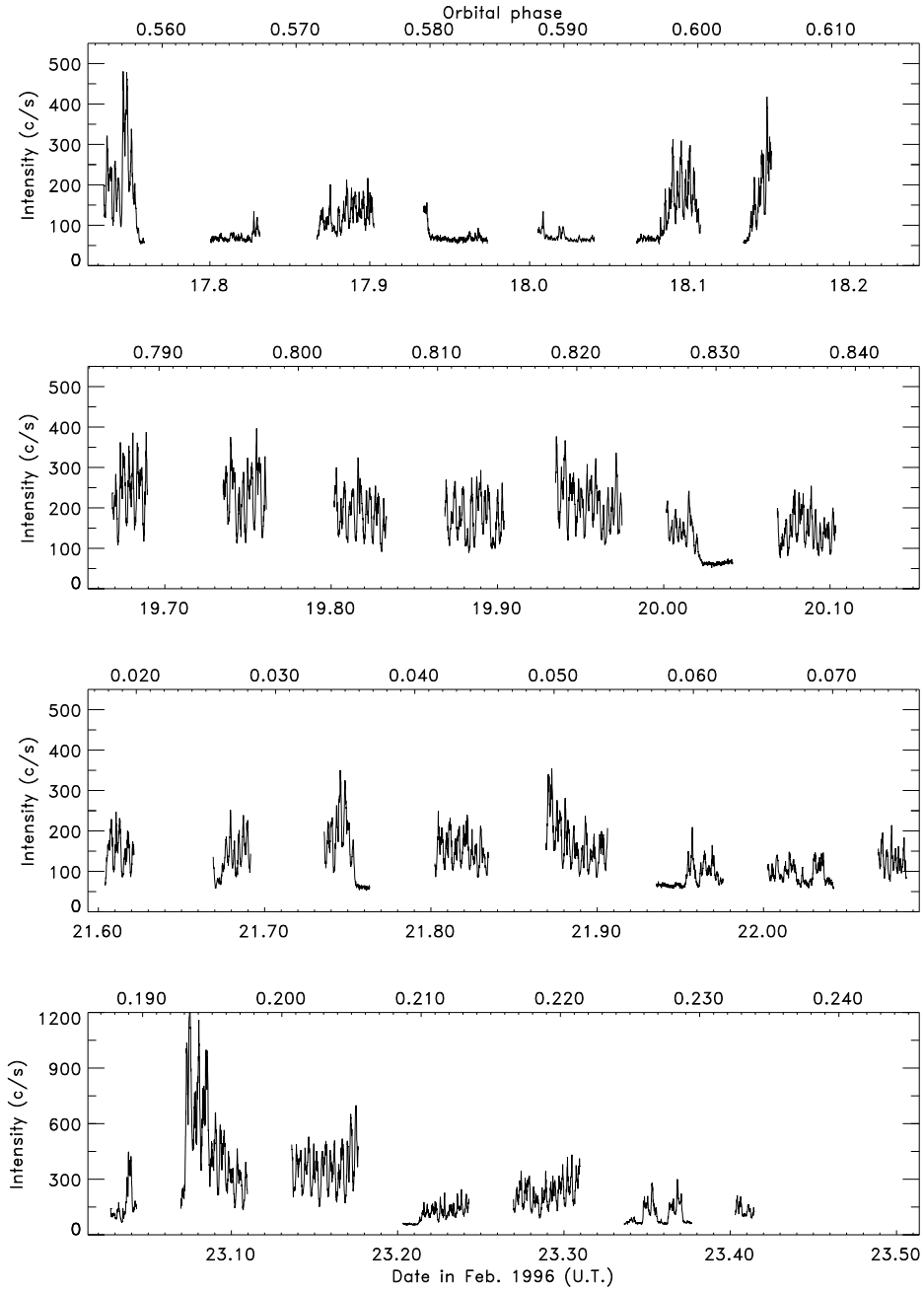
Fig. 1.— Time histories of the raw RXTE-PCA 2 to 15 keV intensity of 4U 1907+09, the bin time is 32 s. The orbital phases are with respect to the epoch of the maximum distance between the pulsar and the solar barycenter
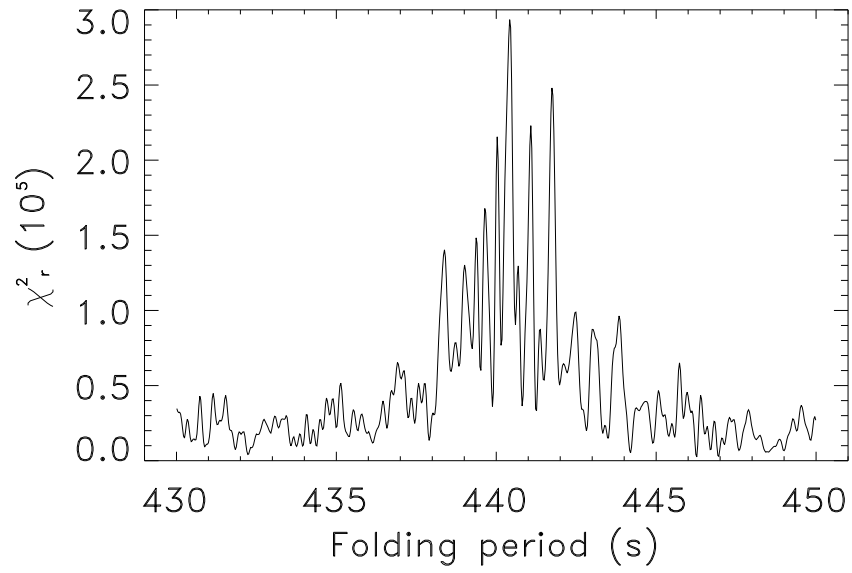
Fig. 2.— Periodogram of the 2 to 15 keV time history data after correction to solar system barycenter but before correction to binary system barycenter
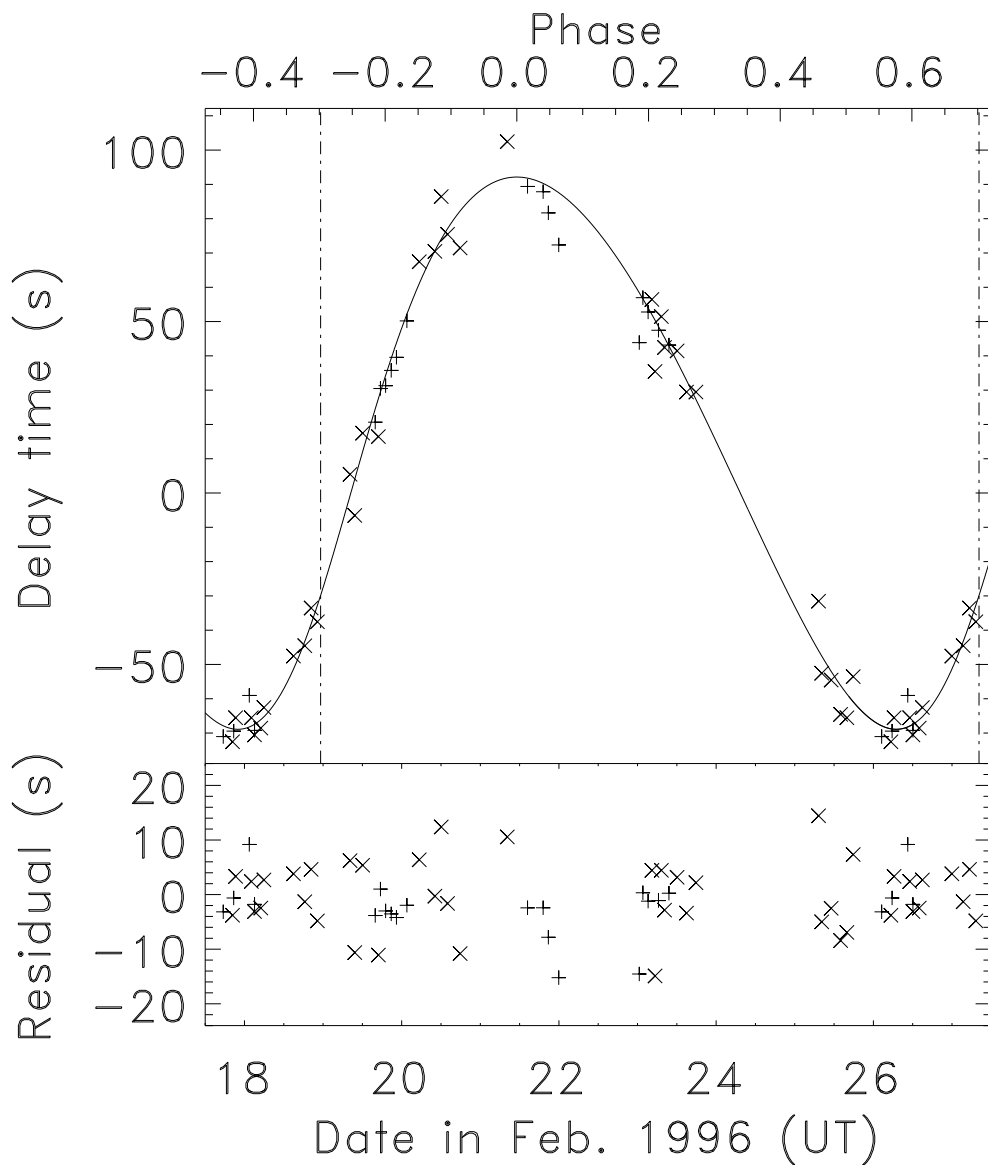
Fig. 3.— The delay time versus time for the RXTE measurements (+ symbols) and for the Tenma measurements folded into the RXTE time of observation (× symbols). The phases indicated on top are with respect to the time of maximum distance between the pulsar and the solar barycenter. The solid line shows the model for the eccentric orbit specified in Table 2. The vertical dashed lines refer to the inferred times of periastron. All data points are repeated modulo $P_{\rm orb}$. The rms of the residuals is 6.6 s
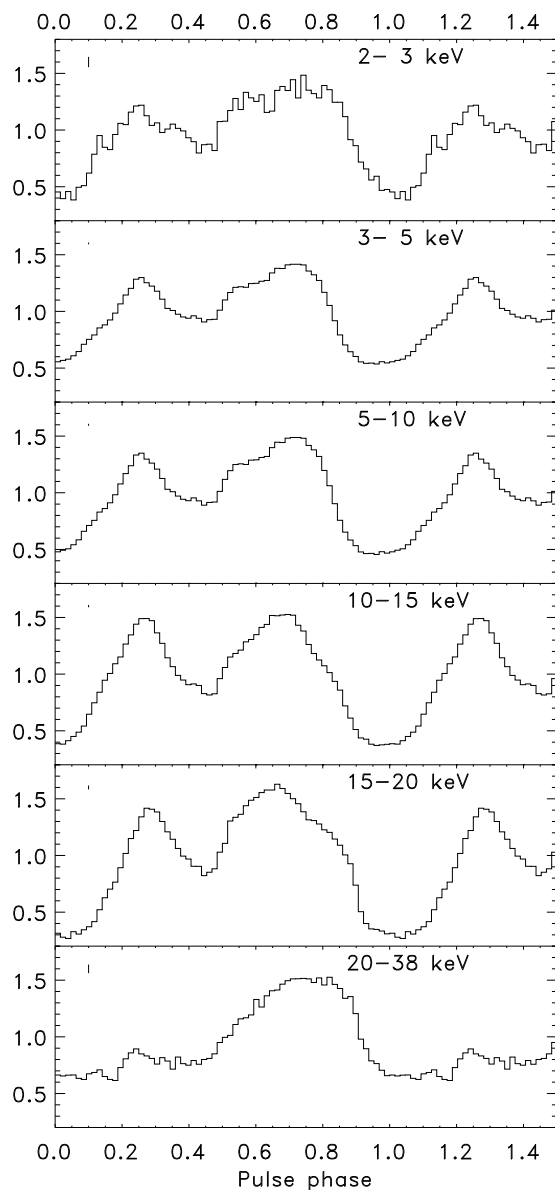
Fig. 4.— The background-subtracted lightcurve folded with the pulse period for 6 bandpasses between 2 and 38 keV. The bandpasses are indicated in each panel as well as the statistical 1σ error in the upper left corner (from top to bottom these errors are equal to 0.045, 0.007, 0.009, 0.010, 0.018 and 0.038). The phase offset is arbitrary. The unit of intensity is the average intensity per bandpass. Only data for 'quiet' periods is used when the source is neither dipping nor flaring above 500 c s^{-1}. The net exposure time for these lightcurves is 29.6 ks out of a total of 79 ks
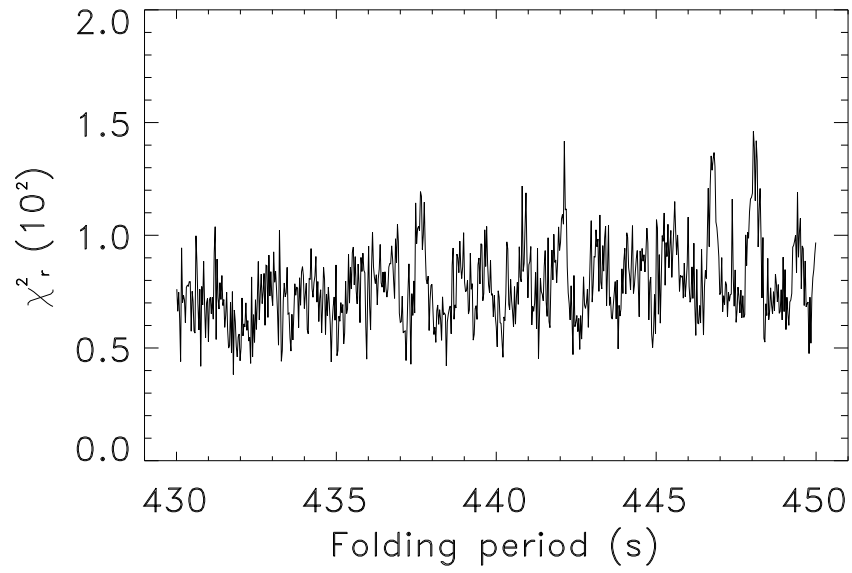
Fig. 5.— Periodogram of the > 40 keV time history data after correction to solar barycenter but before correction to binary barycenter
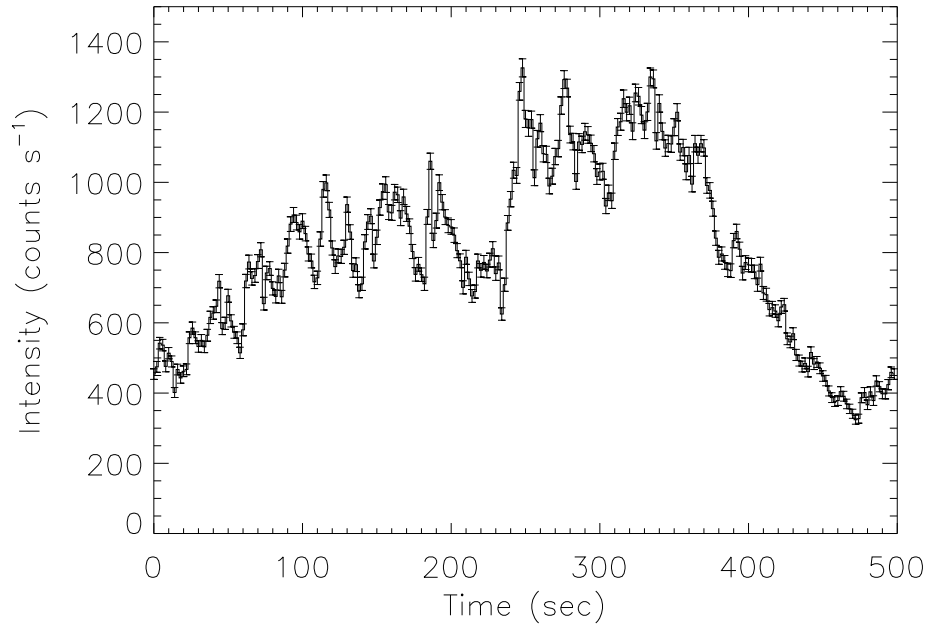
Fig. 6.— An expanded view of the observed X-ray time profile during the secondary flare in the full PCA bandpass. Time is measured from Feb. 23, 1996, 01:56:33 UTC
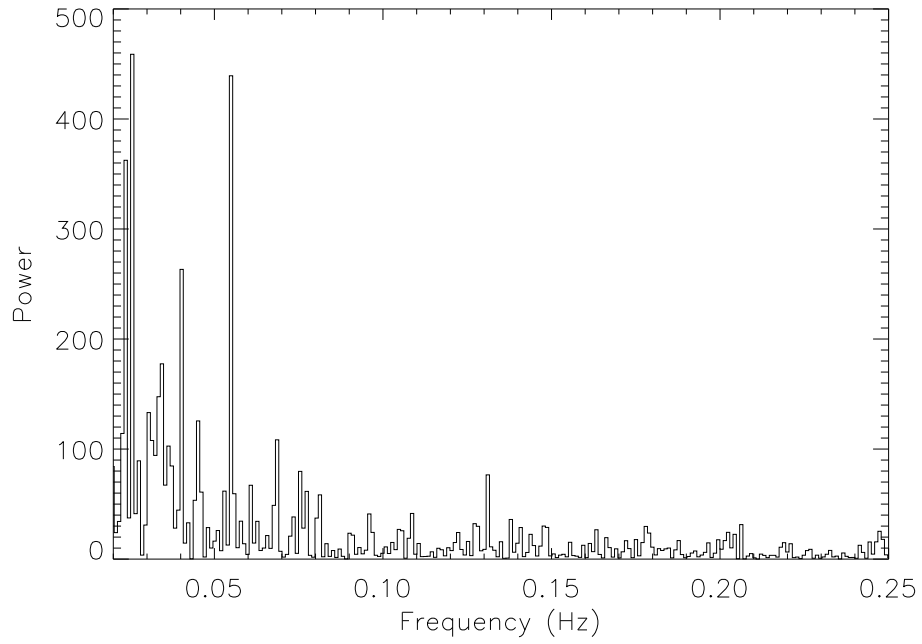
Fig. 7.— The power spectrum of a 1024 s piece of the lightcurve starting 300 s before the start time indicated in figure 6
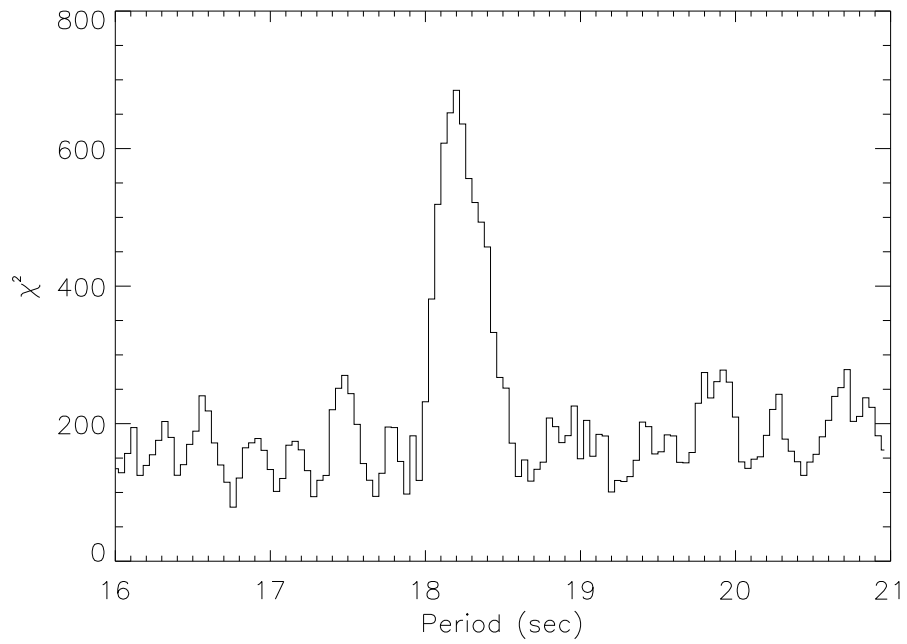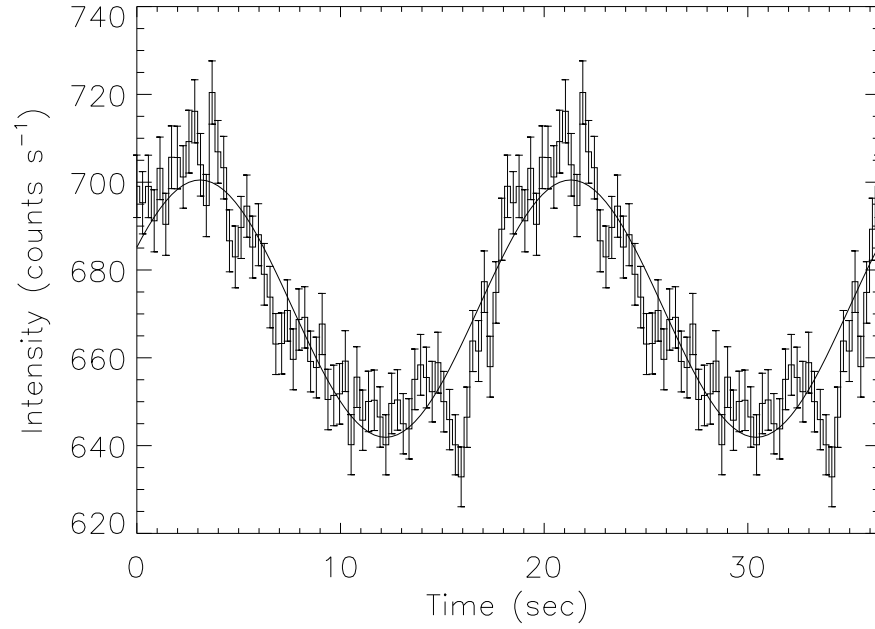
Fig. 8.— Periodogram near 18 s for the flare data

Fig. 9.— Folded background-subtracted lightcurve, folded with a period of 18.2 s, and a sinusoidal fit to the data
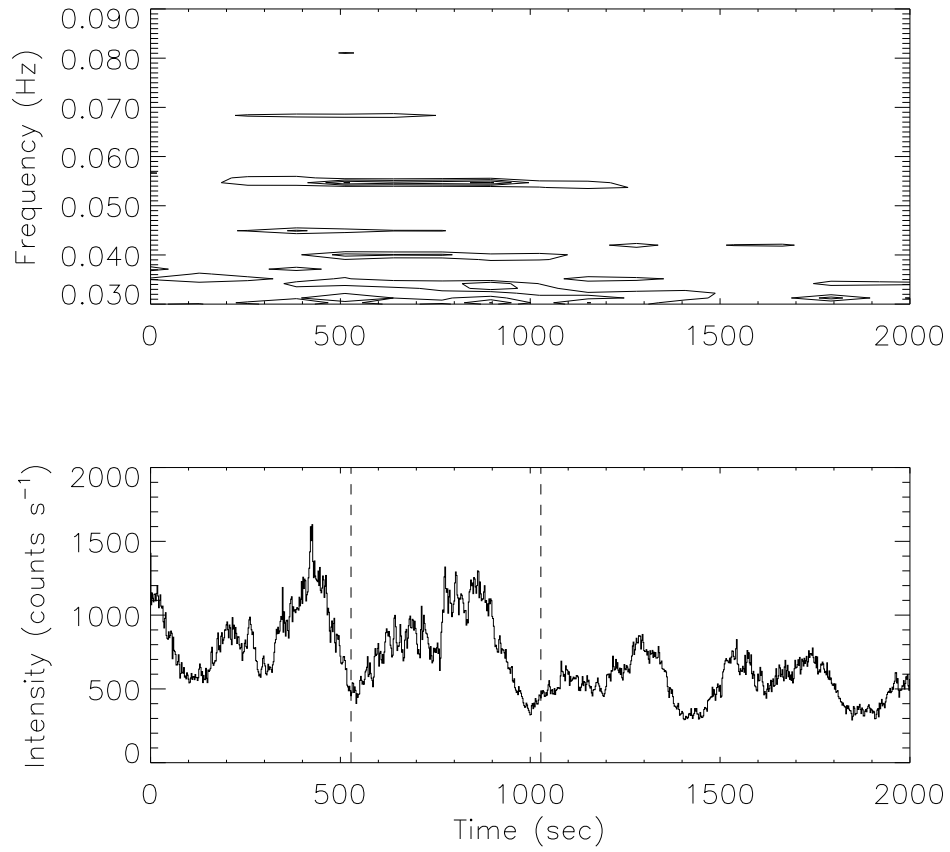
Fig. 10.— The top panel shows a contour map of the dynamic power spectrum. The bottom panel shows the accompanying lightcurve. The vertical dashed lines indicate the time frame of figure 6
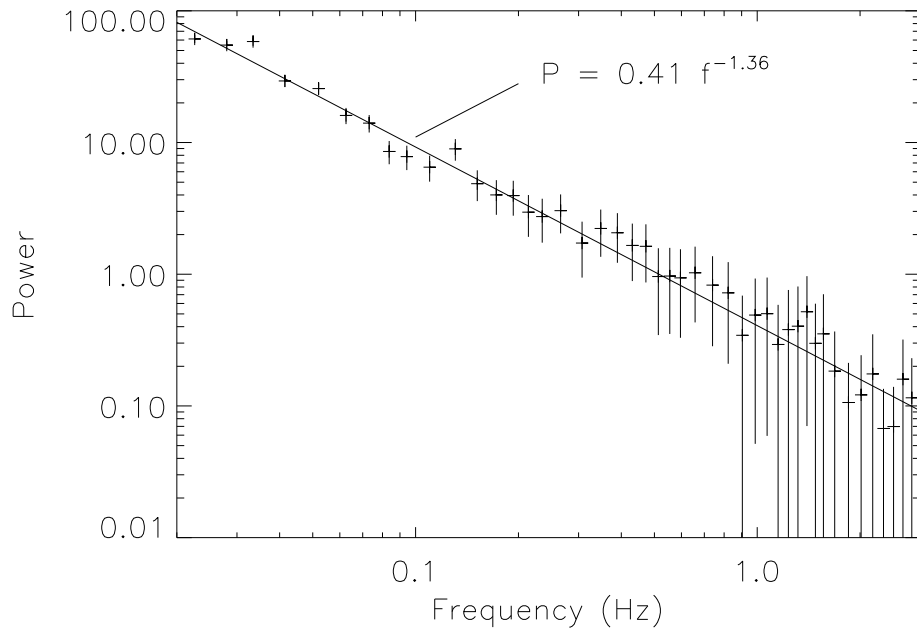
Fig. 11.— The power spectrum of the broadband noise